Desalination and Water Treatment
www.deswater.com

doi: 10.1080/19443994.2013.803330

52 (2014) 3489–3496
May

Taylor & Francis
Taylor & Francis Group

Preparation of zinc tetraaminophthalocyanine sensitized TiO_2 hollow nanospheres and their enhanced photocatalytic properties under visible light

Yinhua Jiang*, Leiqun Guo, Wenli Zhang, Fei Dai, Yun Yan, Fumei Zhang, Hongyan Lv

School of Chemistry and Chemical Engineering, Jiangsu University, Zhenjiang 212013, China
Tel. +86 511 8791928; Fax: +86 511 88791800; email: jyinhua@126.com

Received 17 January 2012; Accepted 24 April 2013

ABSTRACT

A series of zinc tetraaminophthalocyanine (ZnPcN) sensitized TiO_2 hollow nanospheres (ZnPcN/TiO_2) with different loading dosages of ZnPcN were successfully synthesized by a simple immersion method under ultrasonic agitation. The as-prepared ZnPcN/TiO_2 samples were characterized by X-ray diffraction, transmission electron microscopy, field-emission scanning electron microscopy, X-ray energy-dispersive spectrometry, Fourier transform infrared, and ultraviolet–vis diffuse reflectance spectrum. The results show that ZnPcN/TiO_2 nanospheres composed of anatase crystalline phase with hollow structures have obvious absorption in the visible-light region. The photocatalytic activities of ZnPcN/TiO_2 nanospheres were evaluated by degradation of C.I. Basic Blue 41 aqueous solutions with air as an oxidant under visible-light irradiation. The degradation results reveal that the photocatalytic activity of ZnPcN/TiO_2 hollow nanospheres enhances a lot. The apparent rate constant of ZnPcN/TiO_2 nanospheres with the mass ratio of 0.15% between ZnPcN and TiO_2 is almost seven times higher than that of titania hollow nanospheres.

Keywords: TiO_2 hollow nanospheres; Zinc tetraaminophthalocyanine; Sensitization; Visible-light; Photocatalytic activity; Degradation

1. Introduction

In recent years, more and more efforts have been focused on the semiconductor-based photocatalysts for the oxidative degradation of various kinds of organic pollutants [1], and various semiconductors for photocatalysis have been synthesized. TiO_2 is generally used as one of the most popular photocatalysts due to its chemical stability, non-toxicity, inexpensive cost, and high photocatalytic activity [2]. However, TiO_2 can only be excited by ultraviolet (UV) light (wavelength (λ) < 387 nm) due to its wide band-gap (3.2 eV for anatase), which limits its applications in practice [3]. Also, the quantum yield of TiO_2 system for pollutant degradation is usually very low due to the fast recombination of charge carriers. The strategies to enable TiO_2 to harness visible-light for pollutant oxidation by facilitating charge separation includes the following: (1) doping ions (metal [4,5], nonmetal [6] and co-doping [7]), (2) coupling with other semiconductors [8], and (3) loading photosensitizer [9–11]. Among these strategies, using photosensitizer can not only increase the photo

*Corresponding author.

response of TiO_2 to visible-light region due to photosensitizer's strong absorption of solar spectrum, but also enhance the separation efficiency of photoexcited electron–hole pairs in titania [11].

Phthalocyanines and metallo-phthalocyanines are a class of macrocyclic complexes with high photostability and high absorption coefficient in the solar spectrum [12–14], which are often used as photosensitizers to enhance the visible-light photocatalytic activity of TiO_2 in water treatment. For instance, Huo et al. [3] reported the preparation of $CoSPc/TiO_2$/fly-ash cenospheres and found the samples had good catalytic activity under visible light. Sun et al. [11] used aluminum phthalocyanine to sensitize TiO_2 and studied the effect of the experimental parameters on the efficiency for chlorophenol degradation. Mele et al. [15] researched the photocatalytic degradation for 4-nitrophenol by using polycrystalline TiO_2 samples impregnated with Cu(II)-phthalocyanine under visible light. Wang et al. [16] revealed that $CuPcTs/TiO_2$ had higher photocatalytic activity than CuPcTs or pure TiO_2. These above researches all demonstrate that metallo-phthalocyanine or its derivative sensitized TiO_2 nanoparticles can effectively improve the efficiency of organic oxidation under visible light irradiation. However, it is well known that the structure and crystalline size of TiO_2 play important roles in its photocatalytic activity [17,18]. More recently, titania hollow nanosphere, due to its low density, high surface area, good surface permeability as well as large light-harvesting efficiency, has attracted enormous attentions [19–21]. Moreover, titania hollow nanosphere because of its relative large dimension can be easily separated compared with titania nanoparticle. For an environment point of view, metallo-phthalocyanine sensitized TiO_2 hollow nanosphere may be a very useful and efficient visible-light photocatalyst for pollutant treatment. However, few reports have been published on the preparation of metal-phthalocyanines sensitized TiO_2 hollow nanospheres. Herein, we report the synthesis of zinc tetraaminophthalocyanine (ZnPcN) sensitized TiO_2 hollow nanospheres ($ZnPcN/TiO_2$) with different loading dosages of ZnPcN by a simple immersion method under ultrasonic agitation using ZnPcN as a sensitizer. The photocatalytic activity of $ZnPcN/TiO_2$ nanosphere is evaluated by the photocatalytic decomposition of C.I. Basic Blue 41 (CB41) under visible light irradiation ($\lambda > 400$ nm).

2. Experimental

2.1. Material

Tetrabutylorthotitanate ($C_{16}H_{36}O_4Ti$), ethanol, and isopropyl alcohol of analytical reagent grade were purchased from Shanghai Chemical Reagent Company, China. Carbon nanospheres were prepared according to literature procedures [22]. ZnPcN was synthesized, purified, and characterized according to the method of Cong et al. [23]. CB41 dye (purity > 98%) was the commercial product supplied by the dye company and used without further purification. Distilled water was used throughout in all the experiments. The structures of dye CB41 and ZnPcN are given in Fig. 1(a) and (b).

2.2. $ZnPcN/TiO_2$ catalyst preparation

ZnPcN sensitized TiO_2 hollow nanospheres were prepared as follows: Firstly, 0.06 g of carbon nanosphere was added into 80 mL of mixed solution with ethanol and distilled water. Then the mixture was sonicated in an ultrasonic bath under 30 kHz frequencies for 1 h. Next, 10 mL isopropyl alcohol solution containing 0.3 mL tetrabutylorthotitanate ($C_{16}H_{36}O_4Ti$) was dropwise added to the above mixture under vigorous stirring for 30 min. After that, the mixture was kept under reflux condition at 353 K for 6 h to obtain titania coated carbon spheres. Thereafter, the composites were centrifugated, washed, and redispersed in ethanol for three times. After dried at 333 K for 2 h under vacuum, the composites were calcined at 773 K for 3 h in the air to prepare TiO_2 hollow nanospheres. Lastly, 0.1 g of above TiO_2 hollow spheres were dispersed in 50 mL of ethanol containing certain mass of ZnPcN based on the different mass ratios of $ZnPcN/TiO_2$. The mixture was sonicated in an ultrasonic bath under 30 kHz frequencies for 3 h. After that, the mixture was dried at 353 K for 2 h under vacuum to obtain ZnPcN sensitized TiO_2 hollow nanospheres with different dosage of ZnPcN. The as-prepared $ZnPcN/TiO_2$ samples were marked as ZPNT-0.1, ZPNT-0.15, and ZPNT-0.2 in terms of the mass ratios of $ZnPcN/TiO_2$ of 0.1, 0.15 and 0.2%, respectively.

For comparison, TiO_2 nanoparticles were also fabricated in the absence of carbon nanosphere, and the other systhesis conditions were kept the same as those of TiO_2 hollow nanosphere.

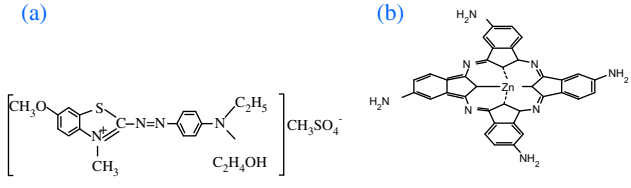

Fig. 1. The chemical structures of CB41 (a) and ZnPcN (b).

2.3. Photocatalysis experiment

The photodegradation reaction of CB41 was conducted in a photocatalytic reactor under visible light at 298 K. The photocatalyst of 50 mg was dispersed in 100 mL 20 mg L^{-1} CB41 aqueous solution. Before illumination, the suspension was magnetically stirred for 30 min in dark to allow the adsorption–desorption equilibrium of CB41 on the catalyst. The photocatalytic reaction was then initiated by irradiating with one 300 W tungsten halogen lamps with a light filter cutting the light below 400 nm. At a defined time interval, 5 mL suspension was withdrawn and centrifuged at 8,000 rpm to remove any suspended solids. Then, the concentration of residual dye CB41 in each sample was measured by a UV–vis spectrophotometer at $\lambda_{max} = 606$ nm.

3. Results and discussion

3.1. Morphology of ZnPcN/TiO_2

Fig. 2 illustrates the typical transmission electron microscopy (TEM) images of TiO_2 nanospheres (a) and ZPNT-0.15 (b). From Fig. 2(a), it can be found that as-prepared TiO_2 obviously owns hollow sphere structure based on the strong contrast between the dark edge and bright center of each sphere. The average diameter of hollow sphere is in the range of 300–350 nm and the shell thickness of sphere is about 35 nm. The TEM image of ZPNT-0.15 (Fig. 2(b)) shows that ZnPcN sensitized TiO_2 still keeps sphericity and hollow structure. However, the contrast between the edge and center of each sphere decreases a little which may be due to the coating of ZnPcN on the surface of TiO_2. ZPNT-0.15 nanosphere has an average diameter of about 300–370 nm and the shell thickness is about 40 nm. These sizes are both slightly increased compared with those of pure TiO_2, which further indicates that ZnPcN has loaded on surfaces of TiO_2 nanospheres.

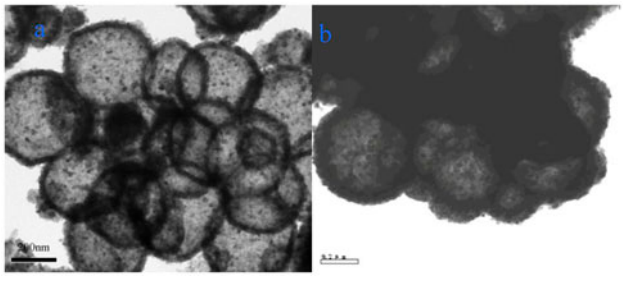

Fig. 2. TEM images of as-prepared TiO_2 hollow sphere (a) and sample ZPNT-0.15 (b).

The corresponding SEM images of TiO_2 nanospheres (a) and ZPNT-0.15 (b) are shown in Fig. 3. From Fig. 3, it is clear that TiO_2 nanospheres are composed of spherical nanoparticle aggregates and the average size of these nanoparticles is about 25–30 nm. Moreover, from the broken sphere in Fig. 3(a), the hollow structure of sphere is very evident. In Fig. 3, it can also be seen that the surfaces of these spheres all seem very crude which indicates that the ZnPcN sensitization has little effect on the roughness of surfaces. It is reported that rough surface can enhance the adsorption and transportation of contaminations [22], thus improving the photocatalytic activity. These results show that ZnPcN sensitized TiO_2 hollow spheres should have high photocatalytic activity.

Fig. 3(c) shows the X-ray energy-dispersive spectrometry (EDS) spectrum of sample ZPNT-0.15. According to the EDS analysis, the spectrum peaks of Zn, Ti, O, C, and N elements can be identified. Ti and O peaks are from TiO_2 spheres, and C, N, and Zn peaks come from the ZnPcN. The existence of Zn, Ti, O, C, and N indicate that the ZnPcN sensitized TiO_2 has been successfully synthesized.

3.2. XRD analysis

The X-ray diffraction (XRD) patterns of as-prepared samples are shown in Fig. 4. From the XRD pattern of TiO_2 hollow spheres, it can be confirmed that as-prepared TiO_2 spheres are identified as anatase

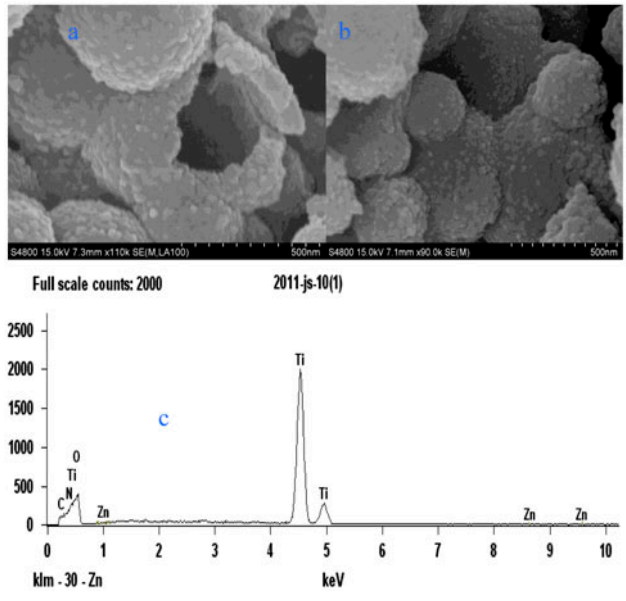

Fig. 3. SEM images of as-prepared TiO_2 hollow sphere (a) and ZPNT-0.15 (b); and the EDS spectrum of ZPNT-0.15 (c).

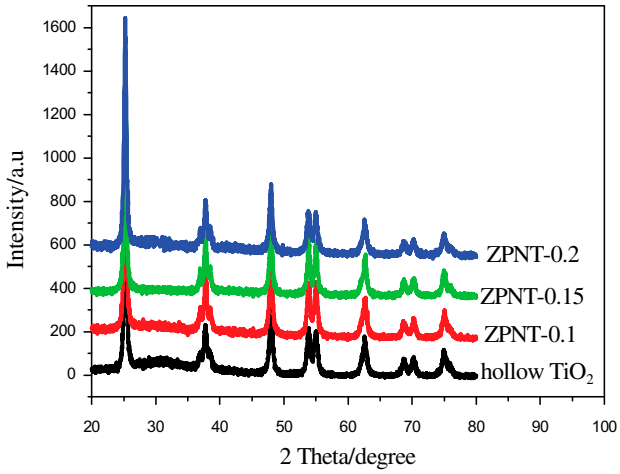

Fig. 4. XRD patterns of different samples.

phase (JCPDS card No. 21-1272), and no other phases of TiO_2, such as rutile or brookite, can be detected via XRD indicating that TiO_2 hollow sphere is composed of pure anatase phase TiO_2. As for the ZnPcN sensitized samples, there is no difference in the patterns of ZnPcN sensitized samples compared with that of TiO_2, and no peaks belonging to ZnPcN have been found due to the small amount of ZnPcN. The results show that the sensitization of ZnPcN does not change the crystalline structure of TiO_2, and ZnPcN molecules do not enter into the lattice of TiO_2.

3.3. UV–vis diffuse reflectance spectra

To study the optical absorption properties of as-synthesized samples, UV–vis diffuse reflectance spectra (DRS) in the range of 200–800 nm were investigated, and the results are shown in Fig. 5. From Fig. 5, it can be seen that ZnPcN sensitized samples all have obvious absorptions in the wavelength of 600–750 nm, which are well corresponding to the Q bands of ZnPcN. However, the reflectance spectrum of TiO_2 shows no absorption in the visible range and only exhibits the fundamental absorption band in the UV region. The result indicates that TiO_2 sensitized with ZnPcN can extend its absorption spectrum into visible light region. The inset figure in Fig. 5 is the UV–vis DRS of ZnPcN sensitized TiO_2 samples in the range of 550–800 nm. The intensity of Q band in the visible range is obviously increased with the increase of ZnPcN dosage. When the mass ratio of ZnPcN and TiO_2 is lower than 0.15%, only the Q band at 692 nm attributed to monomeric ZnPcN species can be found. When the mass ratio is further increased to 0.2%, the Q bands at 692 and 627 nm which belong to the monomeric and dimeric ZnPcN species, respectively, can be easily discovered. The appearance of dimeric peak indicates that the increased dosage of ZnPcN will result in the aggregate of ZnPcN on the surface of TiO_2.

3.4. FTIR spectra

The Fourier transform infrared (FTIR) spectra of ZnPcN, ZnPcN sensitized samples, and TiO_2 hollow sphere are shown in Fig. 6. From the spectrum of the ZnPcN (Fig. 6(a)), the absorption bands at 3,358 and 3,215 cm^{-1} are assigned to OH and N–H stretching vibration, respectively. The 2,920 cm^{-1} band is due to the C–H stretching vibration. The peaks near 1,728 cm^{-1} (C–N bond), 1,612 cm^{-1} (C=C bond),

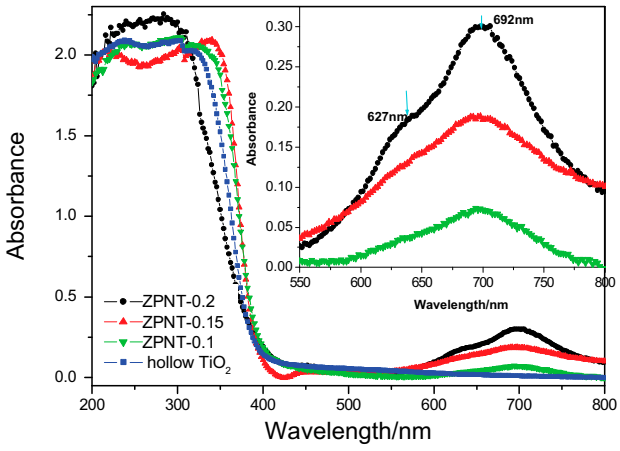

Fig. 5. The UV–vis DRS of different samples; The inset figure is DRS of ZnPcN sensitized TiO_2 samples in the range of 550–800 nm.

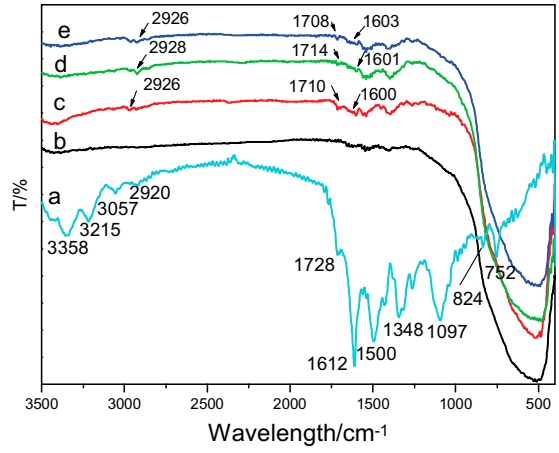

Fig. 6. The FTIR spectra of samples: (a) ZnPcN; (b) TiO_2 hollow sphere; (c) ZPNT-0.1; (d) ZPNT-0.15; and (e) ZPNT-0.2.

1,500 cm^{-1}(C–C bond), and 1,348 cm^{-1} (C=N bond) indicate that there is the ring of phthalocyanine. The characteristic peak of Zn–C is at 824 cm^{-1}. From the spectrum of pure TiO_2 (Fig. 6(b)), the absorption bands in the region of 400–800 cm^{-1} observed in the FTIR are assigned to the stretching vibration of Ti-O. The peaks at 1,623 and 3,376 cm^{-1} are related with the bending vibration and stretching vibration of –OH on the surface of TiO_2, respectively [24], which shows that there contain a great deal of hydroxyls in the hollow TiO_2. In the spectra of ZnPcN sensitized samples (Fig. 6(c)–(e)), except the peaks in the region of 400–800 cm^{-1} (Ti–O), main characteristic peaks near 2,925, 1,710, and 1,600 cm^{-1} assigned to ZnPcN can be clearly observed, which indicates that ZnPcN coupled TiO_2 has been achieved. The attenuation and loss of some peaks from the ZnPcN are probably due to the minor content of ZnPcN in the composite. Moreover, we can also find that these peaks slightly shift compared with those of ZnPcN and 3,215 cm^{-1} assigned to N-H stretching vibrations disappeares which may be covered by the wide and high vibrations OH on the surface of TiO_2 located at 3,390 cm^{-1}. According to the differences in the characteristic peaks of ZnPcN, TiO_2, and ZnPcN/TiO_2, it can be estimated that ZnPcN molecules are anchored onto the surface of the TiO_2 by hydrogen bond between amino groups of ZnPcN and hydroxyls on the surface of TiO_2 hollow spheres.

3.5. Photocatalytic activity

To investigate the photocatalytic activities of ZnPcN sensitized TiO_2 samples, photocatalytic degradation experiments were carried out by degradating CB41 in an aqueous suspension under visible-light irradiation using ZnPcN/TiO_2 samples as photocatalysts. For comparison, the photocatalytic degradation experiment using sample TiO_2 nanoparticle as a photocatalyst was also done. The photodegradation curves were plotted with C/C_0 vs. reaction time "t". C_0 and C are the concentration of dye CB41 in the reaction medium before visible light irradiation (C_0) and after "t" minutes reaction (C), respectively. Fig. 7 shows the CB41 photodegradation curves of samples under the visible-light irradiation. It is obvious that ZnPcN/TiO_2 photocatalysts all exhibit higher activities than pure TiO_2. The corresponding degradation efficiency was calculated from Eq. (1):

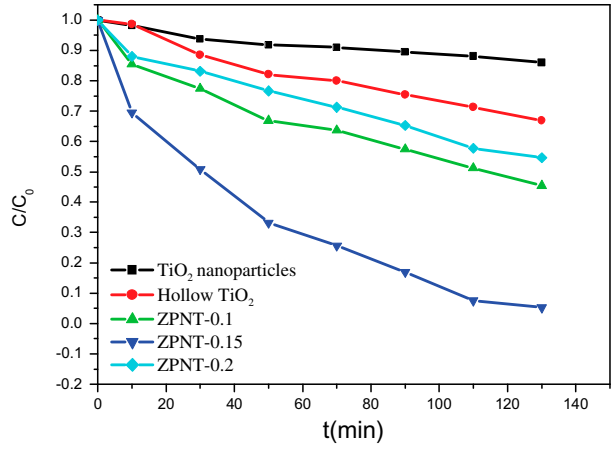

Fig. 7. The CB41 photodegradation curves of samples under the visible-light irradiation.

$$\text{Degradation efficiency} = (C_0 - C)/C_0 \times 100\% \quad (1)$$

The degradation efficiencies of CB41 for sample TiO_2 hollow nanosphere and nanoparticle are about 32.7% and 14.1% after 130 min irradiation, respectively. TiO_2 hollow spheres own better photocatalytic activities than TiO_2 nanoparticles due to their high surface area, which may be beneficial for the surface reaction between O_2 and organic dyes. When the mass ratio between ZnPcN and hollow TiO_2 is 0.1%, the degradation efficiency of CB41 reaches 54.9% at the same irradiation time. As the mass ratio increases to 0.15%, the degradation efficiency of CB41 obviously increases and reaches 94.7%. This may be due to the improvement of ZnPcN dispersion on TiO_2 hollow sphere surfaces (Fig. 3(b)), accordingly, the harvest of light in the region of visible light is significantly increased so as to improve the visible-light photocatalytic activities. However, the degradation efficiency of CB41 reduces to 45.1% when the mass ratio is 0.2%. The reason may be the formation of dimer ZnPcN [25] which lows the quantum efficiency of electric transformation. Thus, ZnPcN cannot effectively sensitize TiO_2 hollow spheres and the degradation rate decreases.

In addition, the kinetic process of CB41 degradation is also investigated. The apparent rate constant (k_{app}) can be chosen as the basic kinetic parameter for the different photocatalysts, since it enables one to determine a photocatalytic activity independent of the previous adsorption period in the dark and the concentration of CB41 which remains in the solution [26]. The apparent first-order kinetic Eq. (2) is used to fit experimental data (Fig. 7):

$$\ln(C_0/C) = k_{app} \times t \quad (2)$$

where k_{app} is the apparent rate constant. By Eq. (2), k_{app} can be calculated from the slopes of the curves of $\ln(C_0/C)$ vs. irradiation time. Fig. 8 shows the linear relationship of $\ln(C_0/C)$ vs. time about the

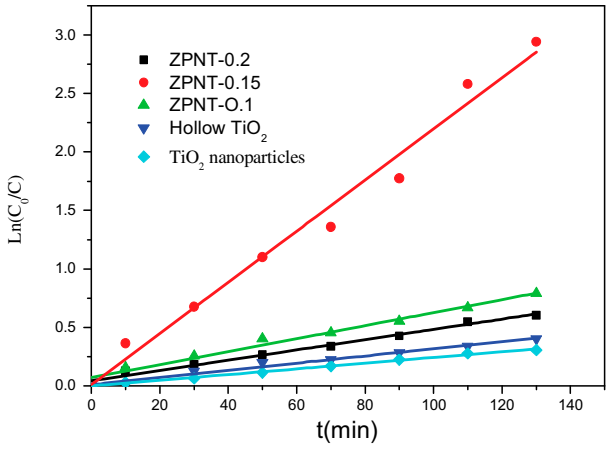

Fig. 8. The linear relationship of ln (C_0/C) vs. time about the photocatalytic degradation of CB41 by all prepared samples.

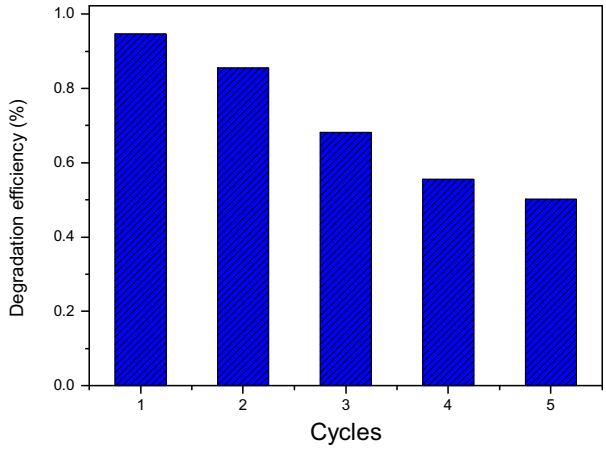

Fig. 9. The recycling experiment of the sample ZPNT-0.15 for CB41 degradation.

photocatalytic degradation of CB41 by all the prepared samples. From Fig. 8, the apparent rate constants of different samples are obtained. k_{app} and linear correlation coefficient of R are listed in Table 1. As seen in Table 1, the apparent rate constants of ZnPcN/TiO_2 samples are all larger than that of pure TiO_2. The apparent rate constant of ZnPcN/TiO_2 hollow nanospheres with the mass ratio of 0.15% between ZnPcN and hollow TiO_2 is almost seven times higher than that of titania hollow nanospheres.

3.6. Catalyst stability

The catalyst stability plays an important role in the practical application of the photocatalyst. The repeated experiments of CB41 degradation for ZnPcN/TiO_2 hollow nanospheres with the mass ratio of 0.15% were conducted. After each run, the photocatalyst was collected, and redispersed into new solution of CB41, followed by equilibrium and visible light irradiation. The results of repeated experiments are shown in Fig. 9. From Fig. 9, it can be found that the photodegradation efficiency of CB41 gradually decreases with the increase of recycling time. Two causes are possible: First, with the recycling time increased, the amount of photocatalysts will be decreased due to filtration and collection. Second, the immobilized ZnPcN on TiO_2 suffers from a gradual bleaching during the photoreaction process [11], which reduces the capture rate of visible-light.

Table 1
Apparent rate constant k_{app} (min^{-1}) and regression relative coefficient R for the TiO_2 nanoparticles, hollow sphere, and ZnPcN/TiO_2 hollow nanosphere

Sample	Apparent rate constant k_{app} (min^{-1})	Regression relative coefficient R
TiO_2 nanoparticles	0.00244	0.996
Hollow TiO_2	0.00306	0.980
ZPNT-0.1	0.00556	0.977
ZPNT-0.15	0.02188	0.980
ZPNT-0.2	0.00440	0.983

3.7. Photocatalytic mechanism of ZnPcN/TiO_2

The photocatalytic mechanism of ZnPcN/TiO_2 under visible light irradiation is photosensitization. The phthalocyanines in the solid state behave as p-type semiconductors, characterized by energy of the band gap about 2 eV [27]. Due to its low band gap, ZnPcN molecules can be easily excited by visible light and generate electrons. Then, the excited electrons transfer to the conduction band of titania due to the energy level of the excited state of the ZnPcN is higher than that of titania conduction band, followed by generation of ZnPcN cation radical ($ZnPcN^{\cdot+}$) and superoxide anion radical ($O_2^{\cdot-}$) in the system. The superoxide anion radical ($O_2^{\cdot-}$) production is essential for inducing the formation of $HO_2^{\cdot}$ and $OH^{\cdot}$ radicals responsible for oxidant attacks to CB41 in photocatalytic reactions [1]. At the same time, $ZnPcN^{\cdot+}$ radical has a high redox potential [28], which can effectively oxidize dye CB41, together with recovery of the original ZnPcN. In this cycle, TiO_2 only acts as an electron mediator, and the ZnPcN works as a sensitizer. Through photosensitization, the quantum yield of the

oxidized and deoxidized process is increased, and thus the degradation rate is improved. However, there exists an optimal phthalocyanine content because too much dosages will result in the formation of dimeric phthalocyanine. The literature has reported that the excited state of the dimer lives much shorter than that of the monomer, not favoring the injection of electron into the conduction band of TiO_2 to generate oxidative species [16]. As a result, the degradation efficiency of CB41 will decrease. According to the data of photocatalytic experiment, we can know that the optimal ZnPcN content is 0.15% (mass percent) to obtain high photocatalytic activity.

4. Conclusion

In this study, ZnPcN sensitized TiO_2 hollow nanospheres (ZnPcN/TiO_2) with different loading dosages of ZnPcN by a simple immersion method under ultrasonic agitation were successfully synthesized. The photocatalytic activity of as-prepared ZnPcN/TiO_2 was determined by degradation of CB41 in aqueous solution under visible light irradiation. Compared with pure titania, ZnPcN/TiO_2 nanospheres exhibites preferable visible-light activities in CB41 degradation. The apparent rate constant of ZnPcN/TiO_2 hollow nanosphere with the mass rate of ZnPcN and TiO_2 of 0.15% is almost seven times higher than that of pure titania hollow sphere. The mechanism is mainly due to the effective electron transfer from the conduction band of ZnPcN to the conduction band of TiO_2, so the quantum yield of the oxidized and deoxidized process is increased, resulting in the high degradation rate. The dosage of ZnPcN is also very important for the photodegradation activity of compound catalyst. Too high dosages of ZnPcN will result in its aggregate, thus decreasing the catalytic activity.

Acknowledgments

This research was sponsored by the National Basic Research Program of China (2007CB936300), research Foundation for Advanced Talents of Jiangsu University (10JDG142) and China Postdoctoral Science Foundation (no.2011M500869).

References

[1] G. Mele, R. Del Sole, G. Vasapollo, E. Garcı´a-López, L. Palmisano, M. Schiavello, Photocatalytic degradation of 4-nitrophenol in aqueous suspension by using polycrystalline TiO_2 impregnated with functionalized Cu(II)–porphyrin or Cu(II)-phthalocyanine, J. Catal. 217 (2003) 334–342.
[2] A. Fujishima, T.N. Rao, D.A. Tryk, Titanium dioxide photocatalysis, J. Photochem. Photobiol. C: Photochem. Rev. 1 (2000) 1–21.
[3] P. Huo, Y. Yan, S. Li, H. Li, W. Huang, Preparation and characterization of Cobalt Sulfophthalocyanine/TiO_2/fly-ash cenospheres photocatalyst and study on degradation activity under visible light, Appl. Surf. Sci. 255 (2009) 6914–6917.
[4] Y. Wang, H. Cheng, L. Zhang, Y. Hao, J. Ma, B. Xu, W. Li, H. Cheng, The preparation, characterization, photoelectrochemical and photocatalytic properties of lanthanide metal-ion-doped TiO_2 nanoparticles, J. Mol. Catal. A: Chem. 151 (2000) 205–216.
[5] S. Leghari, S. Sajjad, F. Chen, J. Zhang, WO_3/TiO_2 composite with morphology change via hydrothermal template-freeroute as an efficient visible light photocatalyst, Chem. Eng. J. 166 (2011) 906–915.
[6] G. Tian, K. Pan, H. Fu, L. Jing, W. Zhou, Enhanced photocatalytic activity of S-doped TiO_2-ZrO_2 nanoparticles under visible-light irradiation, J. Hazard. Mater. 166 (2009) 939–944.
[7] R. Khan, S.W. Kim, T.-J. Kim, C.-M. Nam, Comparative study of the photocatalytic performance of boron-iron Co-doped and boron-doped TiO_2 nanoparticles, Mater. Chem. Phys. 112 (2008) 167–172.
[8] D. Yu, X. Yu, Ch. Wang, X. Liu, Y. Xing, Synthesis of natural cellulose-templated TiO_2/Ag nanosponge composites and photocatalytic properties, Appl. Mater. Interf. 4 (2012) 2781–2787.
[9] R. Gerdes, D. Wöhrle, W. Spiller, G. Schneider, G. Schnurpfeil, G. Schulz-Ekloff, Photo-oxidation of phenol and monochlorophenols in oxygen-saturated aqueous solutions by different photosensitizers, J. Photochem. Photobiol. A: Chem. 111 (1997) 65–74.
[10] M. Gmurek, P. Kubat, J. Mosinger, J. Miller, Comparison of two photosensitizers Al(III) phthalocyanine chloride tetrasulfonic acid and meso-tetrakis(4-sulfonatophenyl)porphyrin in the photooxidation of n-butylparaben, J. Photochem. Photobiol. A: Chem. 223 (2011) 50–56.
[11] Q. Sun, Y. Xu, Sensitization of TiO_2 with aluminum phthalocyanine: factors influencing the efficiency for chlorophenol degradation in water under visible light, J. Phys. Chem. C 113 (2009) 12387–12394.
[12] T. Ogunbayo, T. Nyokong, Phototransformation of 4-nitrophenol using Pd phthalocyanines supported on single walled carbon nanotubes, J. Mol. Catal. A: Chem. 337 (2011) 68–76.
[13] Y. Fang, D. Chen, A novel catalyst of Fe-octacarboxylic acid phthalocyanine supported by attapulgite for degradation of Rhodamine B, Mater. Res. Bull. 45 (2010) 1728–1731.
[14] T. Ogunbayo, T. Nyokong, Photocatalytic transformation of chlorophenols under homogeneous and heterogeneous conditions using palladium octadodecylthio phthalocyanine, J. Mol. Catal. A: Chem. 350 (2011) 49–55.
[15] G. Mele, G. Ciccarella, G. Vasapollo, E. García-López, L. Palmisano, M. Schiavello, Photocatalytic degradation of 4-nitrophenol in aqueous suspension by using polycrystalline TiO_2 samples impregnated with Cu(II)-phthalocyanine, Appl. Catal. B: Environ. 38 (2002) 309–319.
[16] Z. Wang, W. Mao, H. Chen, F. Zhang, X. Fan, G. Qian, Copper(II) phthalocyanine tetrasulfonate sensitized nanocrystalline titania photocatalyst: Synthesis in situ and photocatalysis under visible light, Catal. Commun. 7 (2006) 518–522.
[17] Z. Wu, F. Dong, W. Zhao, H. Wang, Y. Liu, B. Guan, The fabrication and characterization of novel carbon doped TiO_2 nanotubes, nanowires and nanorods with high visible light photocatalytic activity, Nanotechnology 20 (2009) 235701–235711.
[18] M. Inagaki, N. Kondo, R. Nonaka, E. Ito, M. Toyoda, K. Sogabe, T. Tsumura, Structure and photoactivity of titania derived from nanotubes and nanofibers, J. Hazard. Mater. 161 (2009) 1514–1521.
[19] H. Bala, Y. Yu, Y. Zhang, Synthesis and photocatalytic oxidation properties of titania hollow spheres, Mater. Lett. 62 (2008) 2070–2073.

[20] Y. Ao, J. Xu, D. Fu, C. Yuan, A simple method to prepare N-doped titania hollow spheres with high photocatalytic activity under visible light, J. Hazard. Mater. 167 (2009) 413–417.
[21] W. Zhao, L. Feng, R. Yang, J. Zheng, X. Li, Synthesis, characterization, and photocatalytic properties of Ag modified hollow SiO_2/TiO_2 hybrid microspheres, Appl. Catal. B: Environ. 103 (2011) 181–189.
[22] C. Wang, Y. Ao, P. Wang, J. Hou, J. Qian, Preparation, characterization and photocatalytic activity of the neodymium-doped TiO_2 hollow spheres, Appl. Surf. Sci. 257 (2010) 227–231.
[23] F. Cong, B. Ning, Y. Ji, X. Wang, F. Ke, Y. Liu, X. Cui, C. Bin, The facile synthesis and characterization of tetraimido-substituted zinc phthalocyanines, Dyes Pigm. 77 (2008) 686–690.
[24] T. Lopez, E. Ortiz, M. Alvarez, J. Navarrete, J.A. Odriozola, F. Martinez-Ortega, E. Páez-Mozo, P. Escobar, K. Espinoza I. Rivero, Study of the stabilization of zinc phthalocyanine in sol-gel TiO_2 for photodynamic therapy applications. Nanomed.: Nanotechnol. Biol. Med. 6 (2010) 777–785.
[25] L.T. Ueno, A.E.H. Machado, F.B.C. Machado, Theoretical studies of zinc phthalocyanine monomer, dimer and trimer forms, J. Mol. Struct. THEOCHEM 899 (2009) 71–78.
[26] C. Wang, Y. Ao, P. Wang, J. Hou, J. Qian, S. Zhang, Preparation, characterization, photocatalytic properties of titania hollow sphere doped with cerium, J. Hazard. Mater. 178 (2010) 517–521.
[27] V. Iliev, D. Tomova, L. Bilyarska, L. Prahov, L. Petrov, Phthalocyanine modified TiO_2 or WO_3-catalysts for photooxidation of sulfide and thiosulfate ions upon irradiation with visible light, J. Photochem. Photobiol. A: Chem. 159 (2003) 281–287.
[28] J. Hodak, C. Quinteros, M. Litter, E. Roman, Sensitization of TiO_2 with phthalocyanines. Part 1. Photo-oxidations using hydroxoaluminium tricarboxymonoamidephthalocyanine adsorbed on TiO_2, J. Chem. Soc., Faraday Trans. 92 (1996) 5081–5088.